V International Conference on Computational Methods for Coupled Problems in Science and Engineering
COUPLED PROBLEMS 2013
S. Idelsohn, M. Papadrakakis and B. Schrefler (Eds)

TOWARDS INTERACTION OF ELASTIC STRUCTURES WITH TURBULENCE INDUCED ACOUSTICS AT LOW MACH NUMBERS

Frank Flitz[*†] **and Michael Schäfer**[*]

[*]Institute of Numerical Methods in Mechanical Engineering
Technische Universität Darmstadt
Dolivostraße 15, 64293 Darmstadt, Germany
e-mail: {flitz,schaefer}@fnb.tu-darmstadt.de, http://www.fnb.tu-darmstadt.de

[†]Graduate School of Computational Engineering
Technische Universität Darmstadt
Dolivostraße 15, 64293 Darmstadt, Germany
e-mail: flitz@gsc.tu-darmstadt.de, http://www.graduate-school-ce.de

Key words: Acoustics, Fluid-structure interaction (FSI), Splitting approach, Fluid-structure-acoustics interaction

Abstract. We present an approach for fluid-structure-acoustics interaction that aims at the low Mach number range and combines a splitting approach for the fluid, similar to the linearized perturbed compressible equations of Seo and Moon, with a strongly coupled fluid-structure interaction (FSI) concept (split FSI). We compare this approach to an acoustic FSI via a numerical simulation of a vibrational acoustics test case.

1 INTRODUCTION

1.1 Motivation

Combining aeroacoustics and FSI provides a field of interesting applications. One such application, for instance, is the impact of turbulence induced acoustic waves on an elastic structure. For this, an interaction of fluid, structure and acoustics has to be considered.

1.2 State of the art

In the area of fluid-structure-acoustics interaction, which includes the simultaneous treatment of flow induced and vibration induces acoustics, the approaches have different underlying models. The approach with the least modeling uses the compressible Navier-Stokes equations for the fluid. Although there are applications of this approach [1],[2], it is not generally applicable because of its inherent multiscale character [3]. Therefore,

another approach is to incorporate the acoustic analogy of Lighthill [4],[5] together with a one-way coupling from the structure to the acoustics [6],[7]. The approach of Zheng et al. [8] applies a splitting approach for the fluid together with a one-way coupling from the structure to the acoustics as well. No approach with a joint feedback of the incompressible and the acoustic part to the structure is found.

1.3 Procedure

We present an approach for a split FSI (a interaction between a structure and a fluid following a splitting approach) and show its feasibility to reproduce vibrational acoustics via a comparison to an acoustic FSI. In this approach of a split FSI the ability to model aeroacoustics is not harmed.

1.4 Outline

In section 2 the used methods are presented, followed by section 3, where a test case is introduced that illustrates the capabilities of the split FSI. In section 4 the conclusions are drawn.

2 METHODS

The equations for the split fluid as well as for the acoustic fluid are solved in the in-house finite volume solver FASTEST. The structural equations are solved with the finite element solver FEAP. The coupling between the fluid and the structure is implemented in an implicit, strongly coupled way and boundary conformal grids are used.

2.1 Split FSI

The split FSI is realized via a consistent combination of the splitting approach with the FSI.

2.1.1 Splitting approach

The splitting approach is the basis for our fluid model. It originates from Hardin and Pope [9] as *acoustic/viscous splitting* and was improved by Shen and Sørensen [10],[11]. Ewert and Schröder [12], Seo and Moon [13] and Munz et al. [14] proposed further formulations. Here, we use the formulation of Kornhaas [15], which is mainly based on Seo and Moon's *linearized perturbed compressible equations* [13]. Its starting point is the following splitting.

$$\rho = \rho^{\mathrm{f}} + \rho^{\mathrm{a}} \tag{1}$$

$$\boldsymbol{v} = \boldsymbol{v}^{\mathrm{f}} + \boldsymbol{v}^{\mathrm{a}} \tag{2}$$

$$p = p^{\mathrm{f}} + p^{\mathrm{a}} \tag{3}$$

Here ρ, $\boldsymbol{v}$ and p denote density, velocity and pressure, respectively. The indices $(\cdot)^{\mathrm{f}}$ and $(\cdot)^{\mathrm{a}}$ mark the incompressible and the acoustic (or perturbation) variables. The incompressible variables are determined by the incompressible Navier-Stokes equations

$$\nabla \cdot \boldsymbol{v}^{\mathrm{f}} = 0\,, \tag{4}$$

$$\rho^{\mathrm{f}} \left.\frac{\partial \boldsymbol{v}^{\mathrm{f}}}{\partial t}\right|_{\chi} + \rho^{\mathrm{f}} \left(\boldsymbol{v}^{\mathrm{f}} - \boldsymbol{v}^{\mathrm{g}}\right) \cdot \nabla \boldsymbol{v}^{\mathrm{f}} + \mu \nabla^2 \boldsymbol{v}^{\mathrm{f}} - \nabla p^{\mathrm{f}} = \boldsymbol{0}\,, \tag{5}$$

where t denotes the time and μ the dynamic viscosity. We consider the arbitrary Lagrangian Eulerian (ALE) framework (for Details see for instance [16]) for the fluid, with χ being the referential coordinate, together with the grid velocity

$$\boldsymbol{v}^{\mathrm{g}} = \left.\frac{\partial \boldsymbol{x}}{\partial t}\right|_{\chi}\,, \tag{6}$$

with $\boldsymbol{x}$ denoting the spatial coordinate.

Inserting ρ, $\boldsymbol{v}$ and p into the compressible Navier-Stokes equations yields after simplifications [15]:

$$\left.\frac{\partial \rho^{\mathrm{a}}}{\partial t}\right|_{\chi} + \left(\boldsymbol{v}^{\mathrm{f}} - \boldsymbol{v}^{\mathrm{g}}\right) \cdot \nabla \rho^{\mathrm{a}} + \rho^{\mathrm{f}} \nabla \cdot \boldsymbol{v}^{\mathrm{a}} = 0\,, \tag{7}$$

$$\rho^{\mathrm{f}} \left.\frac{\partial \boldsymbol{v}^{\mathrm{a}}}{\partial t}\right|_{\chi} + \rho^{\mathrm{f}} \left(\boldsymbol{v}^{\mathrm{f}} - \boldsymbol{v}^{\mathrm{g}}\right) \cdot \nabla \boldsymbol{v}^{\mathrm{a}} + \nabla p^{\mathrm{a}} = \boldsymbol{0}\,, \tag{8}$$

$$\left.\frac{\partial p^{\mathrm{a}}}{\partial t}\right|_{\chi} + \rho^{\mathrm{f}} c^2 \nabla \cdot \boldsymbol{v}^{\mathrm{a}} + \left(\boldsymbol{v}^{\mathrm{f}} - \boldsymbol{v}^{\mathrm{g}}\right) \cdot \nabla p^{\mathrm{a}} = - \left.\frac{\partial p^{\mathrm{f}}}{\partial t}\right|_{\chi}\,. \tag{9}$$

We utilize this quite rough variant, since we are not interested in the model of the splitting approach itself, but in the consistent application to the FSI.

2.1.2 FSI coupling

As governing equations in the structure we use

$$\rho^{\mathrm{s}} \frac{\mathrm{d}^2 \boldsymbol{u}}{\mathrm{d}t^2} - (\lambda + G)\, \nabla\, (\nabla \cdot \boldsymbol{u}) - G \nabla^2 \boldsymbol{u} = \boldsymbol{0} \tag{10}$$

where ρ^{s} is the density, $\boldsymbol{u}$ the displacement, λ Lamé's first parameter and G Lamé's second parameter, or shear modulus.

The core of the splitting approach (1)–(3) has implications for the boundary conditions and the FSI. On the fluid-structure interface the fluid velocity has to be equal to the structural velocity. Since we consider low Mach number flow, this has to be modeled via the incompressible flow velocity $\boldsymbol{v}^{\mathrm{f}}$.

$$\boldsymbol{v}^{\mathrm{f}} - \boldsymbol{v}^{\mathrm{s}} = \boldsymbol{0} \tag{11}$$

At a wall and at the fluid-structure interface only the acoustic density and the acoustic pressure have to follow the zero gradient condition, while the acoustic velocity has to be set to zero, since the incompressible velocity is already equal to the wall or structural velocity, respectively.

$$\nabla p^{\mathrm{a}} \cdot \boldsymbol{n} = 0 \tag{12}$$

$$\boldsymbol{v}^{\mathrm{a}} \cdot \boldsymbol{n} = 0 \tag{13}$$

$$\nabla \rho^{\mathrm{a}} \cdot \boldsymbol{n} = 0 \tag{14}$$

Note, that (13) is one key point in the consistent application of the splitting approach to FSI.

At the fluid-structure interface additionally to the incompressible flow stress the acoustic pressure has to be considered for the momentum balance.

$$\boldsymbol{\sigma}^{\mathrm{s}} \cdot \boldsymbol{n} = \mu \left(\nabla \boldsymbol{v}^{\mathrm{f}} + \left(\nabla \boldsymbol{v}^{\mathrm{f}} \right)^{\mathrm{T}} \right) \cdot \boldsymbol{n} - p^{\mathrm{f}} \boldsymbol{I} \cdot \boldsymbol{n} - p^{\mathrm{a}} \boldsymbol{I} \cdot \boldsymbol{n} \tag{15}$$

Here, $\boldsymbol{\sigma}^{\mathrm{s}}$ is the Cauchy stress in the structure. Note, that via (15) the feedback of the acoustics to the structure is implemented, which is another key point in the consistent application of the splitting approach to FSI.

2.2 Acoustic FSI

In the applied test case the classical acoustics act as the reference for the splitting approach. To distinguish its variables from the acoustic variables introduced in (7)–(9), we denote the classical acoustics ones with $(\cdot)^{\mathrm{r}}$. In an ALE framework and without a background flow, the governing equations read as

$$\left. \frac{\partial \boldsymbol{v}^{\mathrm{r}}}{\partial t} \right|_{\chi} - \boldsymbol{v}^{\mathrm{g}} \cdot \nabla \boldsymbol{v}^{\mathrm{r}} + \frac{1}{\rho^{\mathrm{f}}} \nabla p^{\mathrm{r}} = \boldsymbol{0} \,, \tag{16}$$

$$\left. \frac{\partial p^{\mathrm{r}}}{\partial t} \right|_{\chi} + \rho^{\mathrm{f}} c^2 \nabla \cdot \boldsymbol{v}^{\mathrm{r}} - \boldsymbol{v}^{\mathrm{g}} \cdot \nabla p^{\mathrm{r}} = 0 \,. \tag{17}$$

For the classical acoustics the boundary conditions at a wall and at the fluid-structure interface are set to

$$\nabla p^{\mathrm{r}} \cdot \boldsymbol{n} = 0 \,, \tag{18}$$

$$\boldsymbol{v}^{\mathrm{r}} \cdot \boldsymbol{n} = \boldsymbol{v}^{\mathrm{g}} \cdot \boldsymbol{n} \,, \tag{19}$$

and the feedback to the structure is described via

$$\boldsymbol{\sigma}^{\mathrm{s}} \cdot \boldsymbol{n} = -p^{\mathrm{r}} \boldsymbol{I} \cdot \boldsymbol{n} \,. \tag{20}$$

3 NUMERICAL INVESTIGATIONS

In this section we illustrate, that the splitting approach, consistently applied to FSI, is capable of simulation of vibrational acoustics.

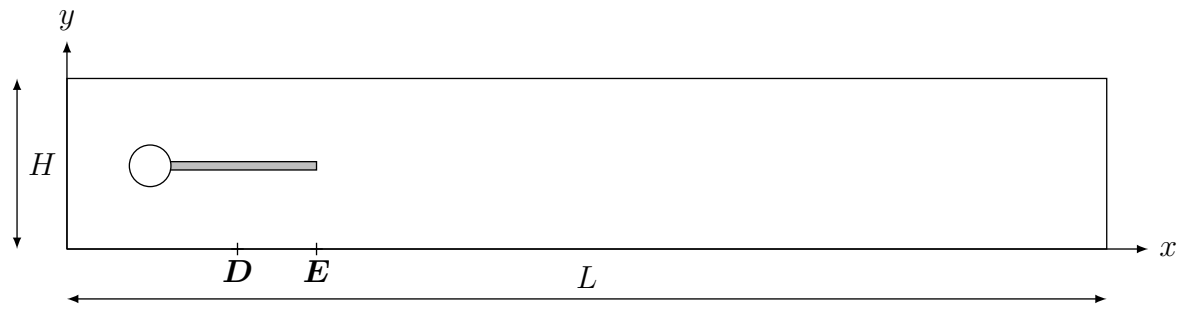

(a) Full domain

(b) Flag detail

Figure 1: Test case setup

3.1 Setup

We adopt the well known FSI benchmark setup from Turek and Hron [17] (figure 1, table 1). We regard the lower and the upper boundary as a wall, the left boundary as a flow wall and acoustic outlet and the right boundary as an outlet. Note, that there is no inflow. We use the material parameters in table 2 for the fluid and the gray indicated flag, while the circle is treated as a rigid body. Initially all variables are set to zero.

Table 1: Geometry parameters

Parameter		Value/m
Channel length	L	2.5
Channel width	H	0.41
Cylinder radius	r	0.05
Flag thickness	h	0.02
Flag tip (at $t = 0$)	A_x	0.6
	A_y	0.2
Circle center	C_x	0.2
	C_y	0.2
Reference point	D_x	0.41
	D_y	0
Reference point	E_x	0.6
	E_y	0

Table 2: Material parameters

Parameter		Value	
Young's modulus	E	0.14	MPa
Poisson's ratio	ν	0.4	
Structural density	ρ^{s}	1×10^{2}	$\mathrm{kg}\frac{1}{\mathrm{m}^3}$
Fluid density	ρ^{f}	1×10^{3}	$\mathrm{kg}\frac{1}{\mathrm{m}^3}$
Dynamic viscosity	μ	1×10^{-3}	$\mathrm{kg}\frac{1}{\mathrm{m\,s}}$
Speed of sound	c	5×10^{-2}	$\mathrm{m}\frac{1}{\mathrm{s}}$

To generate vibrational acoustics we prescribe a boundary movement at the lower boundary between $\boldsymbol{D}$ and $\boldsymbol{E}$ via

$$y = \begin{cases} y_a \sin\left(\pi \frac{x - D_x}{E_x - D_x}\right)^2 \left(\frac{t}{T} - \frac{1}{2\pi} \sin\left(2\pi \frac{t}{T}\right)\right) & \text{if } t < T \\ y_a \sin\left(\pi \frac{x - D_x}{E_x - D_x}\right)^2 & \text{if } t \geq T \end{cases} \tag{21}$$

with $y_a = 0.001\,\mathrm{m}$, $T = 2\,\mathrm{s}$. With a maximal boundary velocity of $\frac{2y_a}{T}$ at $t = \frac{T}{2}$ this results in a Mach number of $Ma = 0.02$ and, with the diameter of the circle, a Reynolds number of $Re = 100$.

3.2 Results

The object of interest is the displacement of the tip of the flag (figure 2). The minor differences between the split FSI and the acoustic FSI are presumably due to the very simplified version of the splitting approach (7)–(9) used here. Note that if we had, in contrast to (15), neglected the feedback from the acoustics part to the structure, we would have gained a very different displacement, due to the immediate response of the flag, caused by the incompressible part.

The contour plots of the split pressure $p = p^{\mathrm{f}} + p^{\mathrm{a}}$ and the acoustic pressure p^{r} in figure 3 underline the generally good agreement. This illustrates that the consistent application of the splitting approach to fluid-structure interaction is capable of simulating vibrational acoustics.

4 CONCLUSIONS

We presented the consistent application of the splitting approach to fluid-structure interaction, enabling the simulation of vibrational acoustics, without restrictions on the aeroacoustics. This makes the split FSI a decent approach for fluid-structure-acoustics interaction.

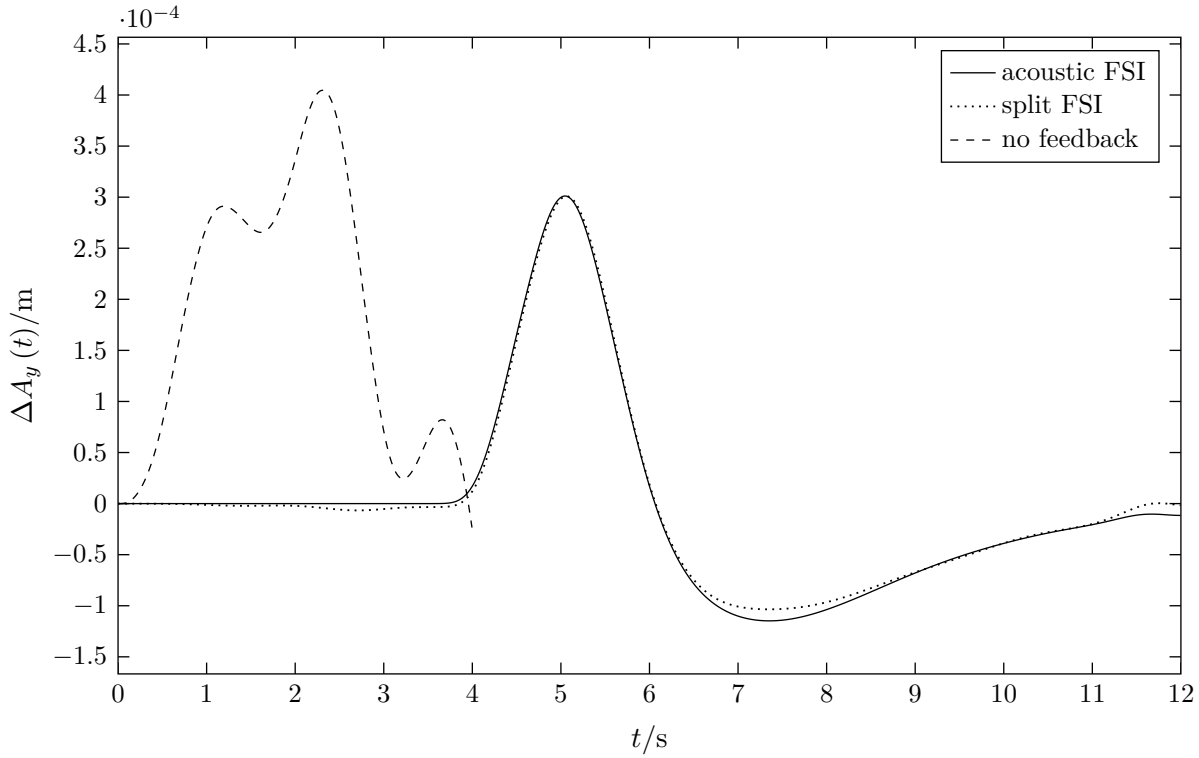

Figure 2: Displacement of the flag tip $\Delta A_y\,(t) = A_y\,(t) - A_y\,(0)$. Until $t = 4\,\mathrm{s}$ additionally to the split FSI and the acoustic FSI the results for the split FSI with absence of feedback from the acoustics to the structure are displayed.

5 ACKNOWLEDGEMENTS

This work was supported by the 'Excellence Initiative' of the German Federal and State Governments and the Graduate School of Computational Engineering at Technische Universität Darmstadt.

REFERENCES

[1] Švancara, P., Horáček, J. and Hrůza, V. Fe modelling of the fluid-structure-acoustic interaction for the vocal folds self-oscillation. In Náprstek, J., Horáček, J., Okrouhlík, M., Marvalová, B., Verhulst, F. and Sawicki, J. T. (eds.) *Vibration Problems ICOVP 2011*, vol. 139 of *Springer Proceedings in Physics*, 801–807 (Springer Netherlands, 2011). `http://dx.doi.org/10.1007/978-94-007-2069-5_108`.

[2] Švancara, P., Horáček, J. and Švec, J. G. Numerical simulation of the self-oscillations of the vocal folds and of the resulting acoustic phenomena in the vocal tract. In Beran, J., Bílek, M., Hejnova, M., Zabka, P. and Ceccarelli, M. (eds.) *Advances in*

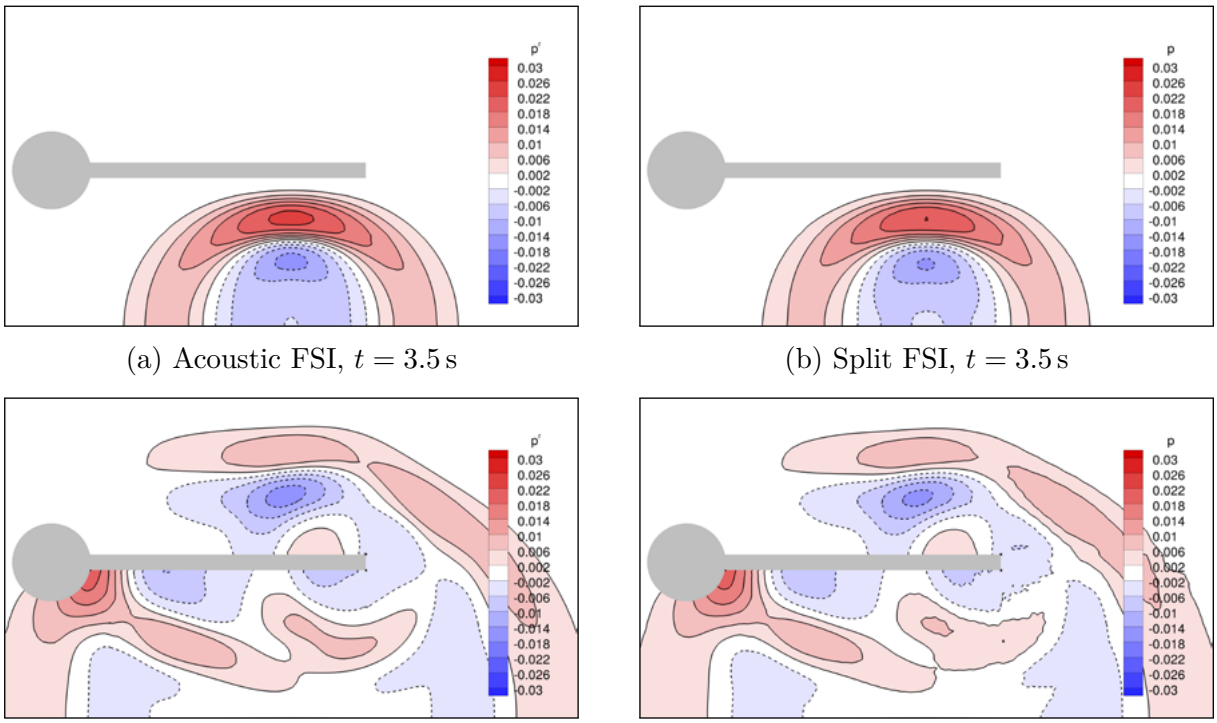

(a) Acoustic FSI, $t = 3.5\,\mathrm{s}$

(b) Split FSI, $t = 3.5\,\mathrm{s}$

(c) Acoustic FSI, $t = 7.0\,\mathrm{s}$

(d) Split FSI, $t = 7.0\,\mathrm{s}$

Figure 3: Contour plots of the split fluid pressure $p = p^{\mathrm{f}} + p^{\mathrm{a}}$ and the acoustic pressure p^{r}

Mechanisms Design, vol. 8 of *Mechanisms and Machine Science*, 357–363 (Springer Netherlands, 2012). http://dx.doi.org/10.1007/978-94-007-5125-5_47.

[3] Wagner, C., Hüttl, T. and Sagaut, P. *Large-Eddy Simulation for Acoustics* (Cambridge University Press, 2007). http://dx.doi.org/10.1017/CBO9780511546143.

[4] Lighthill, M. J. On sound generated aerodynamically. i. general theory. *Proceedings of the Royal Society of London. Series A. Mathematical and Physical Sciences* **211**, 564–587 (1952). http://dx.doi.org/10.1098/rspa.1952.0060.

[5] Lighthill, M. J. On sound generated aerodynamically. ii. turbulence as a source of sound. *Proceedings of the Royal Society of London. Series A. Mathematical and Physical Sciences* **222**, 1–32 (1954). http://dx.doi.org/10.1098/rspa.1954.0049.

[6] Link, G., Kaltenbacher, M., Breuer, M. and Döllinger, M. A 2d finite-element scheme for fluid–solid–acoustic interactions and its application to human phonation. *Computer Methods in Applied Mechanics and Engineering* **198**, 3321 – 3334 (2009). http://dx.doi.org/10.1016/j.cma.2009.06.009.

[7] Schäfer, F., Müller, S., Uffinger, T., Becker, S., Grabinger, J. and Kaltenbacher, M. Fluid-Structure-Acoustics Interaction of the Flow Past a Thin Flexible Structure. *AIAA Journal* **48**, 738–748 (2010). http://dx.doi.org/10.2514/1.40344.

[8] Zheng, T., Tang, S. and Shen, W. Simulation of vortex sound using the viscous/acoustic splitting approach. *Canadian Society for Mechanical Engineering. Transactions* **35**, 39–56 (2011).

[9] Hardin, J. C. and Pope, D. S. An acoustic/viscous splitting technique for computational aeroacoustics. *Theoretical and Computational Fluid Dynamics* **6**, 323–340 (1994). http://dx.doi.org/10.1007/BF00311844.

[10] Shen, W. and Sørensen, J. Comment on the aeroacoustic formulation of hardin and pope. *AIAA Journal* **1**, 141–143 (1999).

[11] Shen, W. and Sørensen, J. Aeroacoustic modelling of low-speed flows. *Theoretical and Computational Fluid Dynamics* **13**, 271–289 (1999). http://dx.doi.org/10.1007/s001620050118.

[12] Ewert, R. and Schröder, W. Acoustic perturbation equations based on flow decomposition via source filtering. *Journal of Computational Physics* **188**, 365–398 (2003). http://dx.doi.org/10.1016/S0021-9991(03)00168-2.

[13] Seo, J. H. and Moon, Y. J. Linearized perturbed compressible equations for low mach number aeroacoustics. *Journal of Computational Physics* **218**, 702 – 719 (2006). http://dx.doi.org/10.1016/j.jcp.2006.03.003.

[14] Munz, C.-D., Dumbser, M. and Roller, S. Linearized acoustic perturbation equations for low mach number flow with variable density and temperature. *Journal of Computational Physics* **224**, 352 – 364 (2007). http://dx.doi.org/10.1016/j.jcp.2007.02.022.

[15] Kornhaas, M. *Effiziente numerische Methoden für die Simulation aeroakustischer Probleme mit kleinen Machzahlen*. Ph.D. thesis, Technische Universität Darmstadt (2012).

[16] Donea, J., Huerta, A., Ponthot, J.-P. and Rodríguez-Ferran, A. *Arbitrary Lagrangian–Eulerian Methods*, chap. 14, 413–437 (John Wiley & Sons, Ltd, 2004). http://dx.doi.org/10.1002/0470091355.ecm009.

[17] Turek, S. and Hron, J. Proposal for numerical benchmarking of fluid-structure interaction between an elastic object and laminar incompressible flow. In Bungartz, H.-J. and Schäfer, M. (eds.) *Fluid-Structure Interaction*, vol. 53 of *Lecture Notes in Computational Science and Engineering*, 371–385 (Springer Berlin Heidelberg, 2006). http://dx.doi.org/10.1007/3-540-34596-5_15.